Application of infrared thermography measurements in thermal diagnostics of the swimming pool

Wykorzystanie badań termowizyjnych do diagnostyki cieplnej hali pływalni

PIOTR CIUMAN

DOI 10.36119/15.2020.5.4

At the stage of designing a ventilation system for a swimming pool, it is difficult to predict with full conviction what thermal and humidity conditions will prevail in the actual facility and what will be the impact of ventilation on its real energy performance. Often it is only during the operation of the swimming pool that a full assessment of its proper functioning takes place. Various research methods can be helpful in this regard: experimental, analytical and simulation methods, using engineering computer software or numerical calculations CFD.
This paper presents thermal imaging research carried out in a real swimming pool, which is a part of experimental research carried out in this facility to evaluate the thermal, humidity and flow conditions and provide data for numerical simulations CFD and their validation. The results of research carried out with other measurement methods were presented in the paper [3].
Keywords: thermography, thermal imaging camera, experimental research, swimming pool

Na etapie projektowania systemu wentylacji hali pływalni trudno jest z pełnym przekonaniem przewidzieć, jakie warunki cieplno-wilgotnościowe będą panowały w zrealizowanym obiekcie oraz jaki będzie wpływ wentylacji na jego rzeczywistą charakterystykę energetyczną. Często dopiero w trakcie eksploatacji hal pływalni następuje pełna ocena poprawności ich działania. Pomocne w tym mogą być różne metody badawcze: eksperymentalne, analityczne i symulacyjne, z wykorzystaniem inżynierskich programów komputerowych lub obliczeń numerycznych CFD.
W niniejszym artykule przedstawiono badania termowizyjne przeprowadzone w rzeczywistej hali pływalni, które stanowią część badań eksperymentalnych wykonanych w tym obiekcie na potrzeby oceny warunków cieplno-wilgotnościowych i przepływowych oraz dostarczających danych do przeprowadzenia analiz i symulacji numerycznych CFD i ich walidacji. Wyniki badań wykonanych innymi metodami pomiarowymi przedstawiono w artykule [3].
Słowa kluczowe: termografia, kamera termowizyjna, badania eksperymentalne, hala pływalni

Introduction

Thermal imaging is a research method based on a remote and non-contact assessment of temperature distribution on the surface of a given body. It consists in detecting, recording and processing the invisible distribution of infrared radiation emitted by every object whose temperature is higher than absolute zero and converting this radiation into visible light. As a result of the visualization of the measured radiation, a thermal image is obtained which reproduces the temperature distribution of the surface of the examined object.

The results of thermal imaging tests can be used where, based on visualization, registration and interpretation of temperature distribution of the tested surfaces, devices or objects can be diagnosed in a non-invasive way, e. g. to detect irregularities in their operation, assess the technical condition of individual elements before repair or assess the quality of the repair performed.

Thermography and thermovision techniques are currently used in almost all areas of research and measurement in the field of the TNDT methods (thermographic non-destructive testing). In addition to many military and scientific applications, they are widely used in medicine, industry, electricity, construction, heating and gas industry. Other important applications include rescue, ecology and hydro-meteorology, and even in geological and space exploration. In connection with recent events around the world, thermal imaging tests are also used to detect people with COVID-19 in public space.

In issues related to thermal physics of buildings, it is useful to know the temperature distribution in the cross-section and on the surfaces of building partitions for their thermal diagnostics, to study the condition of thermal insulation and leakage in partitions and the location of undesirable air infiltration [9, 12, 17]. The common application of thermal imaging tests in construction also includes systems and installations which are technical equipment of buildings. The knowledge of the temperature distribution can be used to assess the thermal insulation condition of the cables and the correct functioning of the central heating system (airlock, leakage, contamination and hydraulic overregulation) and to detect failures of the internal installations [18]. The results of thermal imaging tests can also be used to validate the numerical model. For example, in the research [19], a numerical model of heat exchange through building partitions with elements of central heating system was verified using thermography. The application of thermal imaging research also includes ventilation and air-conditioning systems. For example, it was used to assess the

Piotr Ciuman, PhD – https//orcid.org/0000-0002-2691-1588, Department of Heating, Ventilation and Dust Removal Technology, Silesian University of Technology, Konarskiego 20, 44-100 Gliwice, Poland. Correspondence author/Adres do korespondencji: piotr.ciuman@polsl.pl

airflow from an individual air diffuser based on the temperature distribution in the vertical axis of the supply air jet [1] and to determine the range of the supply air jet based on the temperature distribution of the jet in its entire longitudinal section and the direction of the supply airflow [7], as well as to test air curtains using visualization and recording of airflow in the zone of the greatest influence of the supply air jet [11]. In these cases, thermal imaging measurement was an alternative test method that would traditionally require the measurement of air velocity and temperature at many measurement points, using a large number of sensors, which extends the measurement time and may in some cases be technically unfeasible. Noteworthy is also the research [13], in which thermal imaging tests were used to check the thermal and humidity conditions in the actual, ventilated indoor ice rink, taking into account the possibility of moisture condensation on the internal surfaces of the external walls and ceiling.

In the scope of scientific interests of the author of this paper, there are issues related to modelling of ventilation air distribution in the actual swimming pool [2]. To perform ventilation tests of this facility, including assessment of the microclimate and energy consumption, it was necessary to carry out the experimental research described in the paper [3]. To collect data for thermal diagnostics of the swimming pool and to assess the thermal-humidity and flow conditions occurring in it, additional research was carried out using the thermovision technique, described in this paper.

The data obtained from experimental research (including thermovision) were also used as boundary conditions for the development and validation of the numerical model of the facility, which allowed to conduct multi-variant research on the ventilation of the swimming pool using numerical simulations CFD [2, 4, 6] and was used to perform energy analyses of ventilation processes in this building [5].

Test object

The object of the research was the actual school swimming pool in Gliwice, with the following dimensions: length 17.6 m, width 11.7 m, average height 4.4 m. The external north-western wall of the building was located in the vicinity of old multi-family buildings, and the external south-western wall bordered on the sports field. The external walls of the swimming pool were made of silicate brick, polystyrene and hollow brick. The north-western wall was additionally plastered on the outside. In the south-western wall, there were six windows with the following dimensions: length 2.65 m and height 2.58 m. These were PVC windows with double glazing, equipped with remote-controlled external blinds. The internal partitions of the examined swimming pool were: the north-eastern wall, which bordered the locker room, the south-eastern wall, adjacent to the sports hall, the swimming pool floor, under which there was a basement, and the ceiling, above which there was an unheated attic. Since the construction of the facility a partial thermo-modernisation was carried out, but there was a lack of precise information in this respect. Therefore, the available technical documentation was not up-to-date.

The swimming pool was equipped with a central heating system, powered from the municipal heating network. Six radiators were located under the windows in the south-western wall, and another two radiators were located near the north-western wall.

The lighting of the swimming pool was provided by eight halogen lamps located under the ceiling – four lamps at each side of the longer walls.

The thermal and humidity conditions inside the swimming pool were maintained using a fully-air mechanical ventilation system. The system operated continuously, supplying the same airflow around the clock. The swimming pool was equipped with a mixing ventilation system with one-sided, under-window air supply. In addition, a ceiling air supply was used on the opposite side of the facility at the locker room exit. The exhaust air was extracted under the ceiling of the room.

Fig. 1 shows the interior of the examined swimming pool. The location of ceiling supply grilles, slot diffusers and exhaust grilles is marked on it. Fig. 2 shows the arrangement of O1-O6 windows in the south-western wall, K1-K7 ceiling supply grilles and N1-N12 slot diffusers.

Research methodology

In order to use the emission of infrared radiation in the research of temperature distribution on the surface of a real object it is necessary to introduce a model with ideal radiation properties, the so-called perfect blackbody with a temperature of T, which according to Stefan-Boltzmann's law emits energy from its surface in the form of heat in an amount:

$$E = \sigma T^4 \qquad (1)$$

where: E [W/m^2] - radiation power, σ - Stefan-Boltzmann constant $\sigma = 5.67 \cdot 10^{-8}$ W/(m^{2}K^4), T [K] - surface temperature.

The actual objects more or less deviate from this model and therefore this devia-

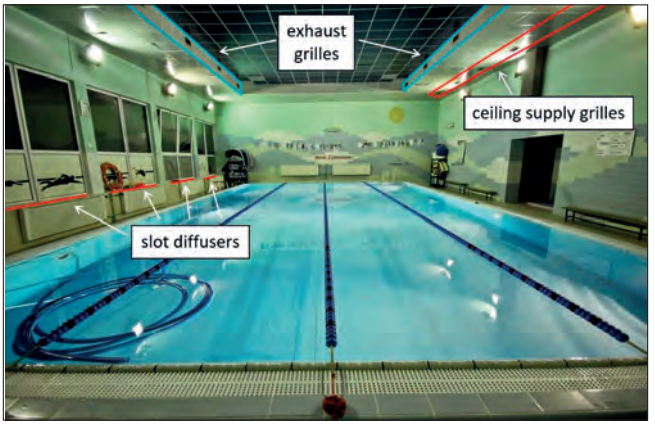

Fig. 1.
View of the interior of the school's swimming pool [21]
Rys. 1. Widok wnętrza badanej hali szkolnej pływalni [21]

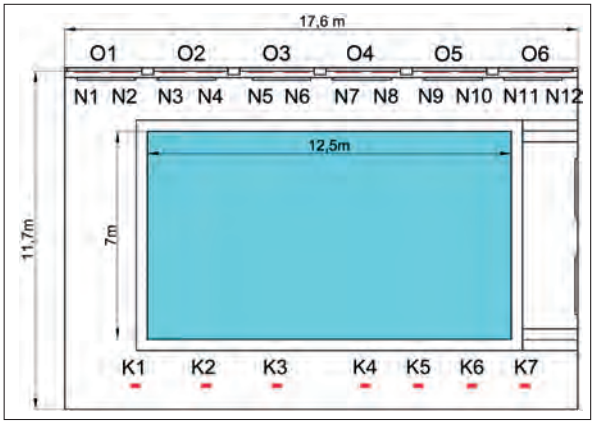

Fig. 2.
Arrangement of ceiling supply grilles, slot diffusers and windows in the swimming pool [2]
Rys. 2. Rozmieszczenie okien oraz nawiewników sufitowych i szczelinowych w hali pływalni [2]

tion is taken into account for thermovision measurements by introducing the emissivity factor of the examined surface. Formula (1) then takes the following form:

$$E = \varepsilon\sigma T^4 \quad (2)$$

Emissivity is a measure of the intensity of radiation emitted from an object in relation to the intensity of radiation emitted from a perfect blackbody of the same temperature. Emissivity for a perfect blackbody would be unity and for real bodies is in the range of $0 < \varepsilon < 1$ and depends primarily on the type of material, its condition, colour and surface temperature, as well as the wavelength and angle of incidence. For example, for typical building materials its value is on average $\varepsilon = 0.7$ - 0.95, and for polished surfaces of gold or other noble materials, its value is the smallest ($\varepsilon = 0.02$ - 0.06).

Thermal imaging tests in the swimming pool (Fig. 1) were conducted on 25 February 2016. Additionally, on that day, the following measurements were carried out: outdoor and supply air parameters, indoor air parameters above the pool basin and around it, water temperature. These measurements were conducted with other measuring instruments and were described in detail in the paper [3].

The scope of thermal imaging research included determination of temperature distribution on internal and external surfaces of building partitions, the examination of the risk of moisture condensation on window surfaces and indirect determination of thermal transmittance of external partitions. The results of this research were needed for the assessment of thermal-humidity conditions and as boundary conditions for numerical simulations and energy analyses.

The methodology of thermal imaging tests

The measurements were carried out with FLIR i50 and ThermaCAM E45 thermal imaging cameras (Fig. 3). Table 1 shows the basic parameters of the thermal imaging cameras used.

Thermal imaging measurements were carried out in accordance with the requirements of the standard [14]. The conditions under which they were carried out are summarised in Table 2. In accordance with the recommendations of the standard, they were conducted during high cloudiness of the sky, at practically windless weather, constant outdoor air temperature and no precipitation. The measurements were carried out from 7:00 to 8:30, thus ensuring that for a minimum period of 12 hours before the start of the inspection the surfaces of the examined partitions were not exposed to sunlight and the outdoor air temperature at that time only slightly differed from the air temperature during the measurements. In addition, the temperature difference between the inside and outside of the swimming pool was greater than 15 K, which is particularly important in the thermography of buildings. This condition is necessary for the correct interpretation of thermograms, to ensure sufficient thermal contrast and proper evaluation of the temperature of areas where damage to the thermal insulation of the building may occur.

Temperature distribution on the surfaces of the examined building partitions was determined with the use of FLIR Tools software [22], which enables edition of thermograms and their adaptation to the needs of the user. For each thermogram, the following parameters were set: emissivity, reflected temperature, distance, air temperature, temperature of the external optics, transmission of the external optics and air relative humidity. Then, by changing the colour palette and temperature scale, it was possible to adjust the thermogram to one's own needs, i.e. to the range that occurred in the examined measurement area. In addition, a dew point alarm was applied in the FLIR Tools software to check the possibility of moisture condensation on windows surfaces.

Methodology for determining thermal transmittance of building partitions

The method described in the paper [20] was used to determine the thermal transmittance of building partitions using thermovision measurements. In this method a one-dimensional model of fixed heat flow through the building envelope was assumed, in which there w an equality of the flux penetrating through the envelope and the fluxes entering from the indoor environment to the envelope and discharged from the envelope to the outdoor environment according to the equation:

$$q = U(T_i - T_e) = \alpha_i(T_i - T_w) = \alpha_e(T_z - T_e) \quad (3)$$

where: U [W/(m^2·K)] – thermal transmittance of building partition, α_i, α_e [W/(m^2·K)] – surface heat transfer coefficient, respectively: of the internal and external surface of partition, T_i, T_e, T_w, T_z [°C or K] – temperature, respectively: of indoor air, outdoor air, internal partition surface and external partition surface.

In the process of penetration, heat is transferred by convection and radiation, so the internal and external surface heat transfer coefficients α_i and α_e are the sums of the coefficients of heat transfer through convection and radiation.

The radiative surface heat transfer coefficient of the external surface of the

Fig. 3.
Thermal imaging cameras used in the tests:
a) FLIR i50;
b) ThermaCAM E45
Rys. 3. Kamery termowizyjne zastosowane w badaniach: a) FLIR i50; b) ThermaCAM E45

Tab. 1. Parameters of thermal imaging cameras used [22]
Tab. 1. Parametry zastosowanych kamer termowizyjnych [22]

FLIR thermal inmaging camera	i50	ThermaCam E45
Detector resolution	140 x 140 pixels	160 x 120 pixels
Field of vision (FOV)	25° x 25° / 0.1 m	34° x 25° / 0.1 m
Temperature measurement range	-20°C ÷ 350°C	-20°C ÷ 250°C
Accuracy of temperature measurement	±2°C or ±2% readings	±2°C or ±2% readings
Thermal sensitivity	<0.1°C in 25°C	0.1°C in 25°C
Radiation spectrum range	7.5 µm ÷ 13 µm	7.5 µm ÷ 13 µm

Tab. 2. Conditions diuring thermovision measurements
Tab. 2. Warunki wykonywania pomiarów termowizyjnych

No.	Parameter	Symbol	Unit	Value
1	Indoor air temperature	T_i	°C	27,4
2	Outdoor air temperature	T_e	°C	0,2
3	Wind speed	v	m/s	0,4
4	Indoor air relative humidity	φ_i	%	56
5	Outdoor air relative humidity	φ_i	%	80

partition takes into account the temperature T_z and the emissivity ε of the external surface of the partition, the reference temperature T_r and the Stefan-Boltzmann constant $\sigma = 5.67 \cdot 10^{-8}$ W/(m^2·K^4) and can be described by an equation [20]:

$$\alpha_{r,e} = \varepsilon\sigma(T_z + T_r)(T_z^2 + T_r^2) \quad (4)$$

where the temperature is expressed in K.

The reference temperature T_r in the equation depends on atmospheric conditions (air temperature and cloud cover) and is not the ambient temperature in close proximity to the building. In the case of thermovision research in an open space, the environment of the object is the space of the sky and the earth's surface (possibly with building elements, usually of different temperature). The paper [8] presents the method of determining the equivalent radiation ambient temperature (reference) for thermovision measurements in an open space and the method of measuring the apparent temperature of the sky necessary for its determination. This method neglects the influence of atmospheric air radiation and the absorption in this air of radiation coming from the examined surface and surfaces of surrounding elements. When a thermal imaging camera is used, the measurements are carried out at short distances from the building envelope and a radiative emission flux (called brightness) is added to the camera lens, consisting of the emission of its surface and the ambient radiation reflected from that surface. The graphs included in the paper [8] enable determination of equivalent ambient temperature for surfaces with different geometrical orientation in relation to the sky and ground surface and are useful in thermovision diagnostics of a building, including building partitions with a different slope of the surface (e.g. a roof).

The radiative surface heat transfer coefficient of the internal surface of the external partition takes into account the transmission of heat by radiation through heat sources such as radiators or partitions of higher temperature. On the other hand, since the interior of the facility is not an infinitely large space and the air emissivity is considered to be equal to zero, there is no radiative heat exchange between the air and the partition. The radiative surface heat transfer coefficient of the internal surface of the external partition takes into account the indoor air temperature T_i, the internal surface temperature of the partition T_w and the Stefan-Boltzmann constant σ and can be described by the equation [20]:

$$\alpha_{r,i} = \sigma(T_i + T_w)(T_i^2 + T_w^2) \approx 4\sigma T_m^3 \quad (5)$$

where T_m is the mean value of the temperature T_i and T_w expressed in K.

The convective heat flux depends on the type of airflow (laminar or turbulent) near the surface of the building envelope. In the case of the external surface of the partition, the convective surface heat transfer coefficient takes into account the turbulent airflow (forced convection) and is dependent on the outdoor air temperature T_e, the temperature of the external surface of the partition T_z and the average air velocity outside the boundary layer of the partition v_∞ (away from the building). For forced, turbulent airflow around a building with a temperature of about 0°C (recommended for thermal imaging tests in construction), the convective surface heat transfer coefficient can be calculated depending on the height of the building wall, according to the formulas [20]:

– for a wall about 30 m high

$$\alpha_{k,e} = 3{,}21 v_\infty^{4/5} \quad (6)$$

– for a wall between 5 and 7 m high (e.g. for single-family buildings)

$$\alpha_{k,e} = 4{,}43 v_\infty^{4/5} \quad (7)$$

The convective surface heat transfer coefficient of the internal surface of the external partition takes into account the laminar or turbulent airflow (natural convection) and is dependent on the indoor air temperature T_i and the internal surface temperature of the partition T_w. This coefficient can be calculated depending on the height of the partition, according to formulas [20]:

– for high objects with a height of > 2. 9 m (turbulent flow)

$$\alpha_{k,i} = 1{,}65(T_i - T_w)^{1/3} \quad (8)$$

– for low objects with a height of < 2. 9 m (laminar flow)

$$\alpha_{k,i} = 1{,}42(T_i - T_w)^{1/4} \quad (9)$$

In the paper [20], formulas for determining the density of the heat flux emitted by the partition to the environment taking into account radiation and forced convection are given:

$$q = \varepsilon\sigma(T_z^4 + T_r^4) + 4{,}43 v_\infty^{4/5}(T_z - T_e) \quad (10)$$

and to determine the density of heat flux absorbed by the partition from the space, taking into account radiation and natural convection:

$$q = \varepsilon\sigma(T_i^4 + T_w^4) + 1{,}65(T_i - T_w)^{4/3} \quad (11)$$

In formulas (10) and (11) the substitute radiative and convective surface heat transfer coefficients of the external and internal surface of the building envelope are taken into account.

Using equations (3), (10) and (11), it is possible to determine the value of thermal transmittance of a building partition U taking into account convection and radiation according to the following formulas:

– using outdoor parameters

$$U = \frac{\varepsilon\sigma\left(T_z^4 - T_r^4\right) + 4{,}43 v_\infty^{4/5}\left(T_z - T_e\right)}{T_i - T_e} \quad (12)$$

– using indoor parameters

$$U = \frac{\varepsilon\sigma\left(T_i^4 - T_w^4\right) + 1{,}65\left(T_i - T_e\right)^{4/3}}{T_i - T_e} \quad (13)$$

The necessary values of temperature on the internal and external surfaces of the partition can be determined using a thermal imaging camera and, on the basis of dependencies (12) and (13), thermal transmittance values can be estimated.

The practice of thermovision measurements shows that the thermal transmittance determined from formulas (12) and (13) may vary due to temperature measurement errors on both sides of the partition and to the fact that the transient heat transfer in the partition occurs due to transport delays, heterogeneous or multilayer structure of the partition, discontinuity of insulation and thermal bridges. Moreover, estimation of the value of surface heat transfer coefficient of the external surface of the partition $_e$ is burdened with errors resulting mainly from changing weather conditions and omitting the influence of solar radiation, humidity and pressure.

Therefore, the methodology of determining the thermal transmittance of a building partition based on thermovision measurements, presented in the paper [20], consists in determining the value of this coefficient as an arithmetic mean of coefficients determined for indoor and outdoor parameters according to formulas (12) and (13).

Results of thermal imaging measurements

The aim of the experimental research carried out in the swimming pool, including thermovision research, was to identify the thermal-humidity conditions prevailing inside the facility. The measurement results were used to determine the thermal transmittance of external partitions and to examine the possibility of moisture condensation on the internal surfaces of windows.

Using thermovision measurements of temperature on the external and internal surfaces of building partitions the values of thermal transmittance were calculated on the basis of formulas (12) and (13), which was purposeful due to the lack of current

building documentation. Since its construction, the swimming pool was subject to random thermomodernisation, but there was no data on the thermal transmittance of the windows and no precise information on the insulation of external walls.

The results of thermovision research were also used to validate the numerical model by comparing the calculated and measured temperature distributions on the internal surfaces of building partitions [2, 4].

Temperature distribution on internal surfaces of building partitions

The first part of the thermal imaging research was the analysis of temperature distribution on the internal surfaces of the building partitions of the examined swimming pool, needed to indirectly determine the thermal transmittance of external walls and windows and to validate the numerical model [2, 4].

Fig. 4 shows the thermogram of the internal surface of the north-western external wall. Two measurement areas were applied in order to determine the temperature of that part of the partition which was not influenced by the radiators. The average temperature of the internal surface of the partition was 26.4°C.

Another thermogram (Fig. 5) shows the internal north-eastern wall, bordering on the swimming pool locker rooms. A single measurement area was applied covering a significant part of the wall, excluding heated lighting lamps. The average temperature of the partition surface was 27.8°C.

On the next thermogram (Fig. 6) the south-eastern internal wall bordering the sports hall is presented. Two measurement areas were applied, which are outside the influence of heated lighting lamps. The average temperature of the partition surface was 27°C.

The thermogram of the internal surface of the south-western external wall with windows is shown in Fig. 8b.

All examined surfaces of partitions were characterized by a similar temperature distribution. The internal surfaces of external walls had a lower temperature than those of the internal walls. The lowest temperature of 24.9°C was obtained for the internal surface of the external wall with windows (outside the area under radiators influence the wall surface temperature was 23.9°C). The highest temperature of 27.8°C was obtained on the internal wall bordering the locker rooms. The air temperature in the locker rooms was comparable to the air temperature in the swimming pool.

Testing the possibility of moisture condensation on the surfaces of the windows in the swimming pool

In swimming pools, due to high humidity gains, it is necessary to ensure such thermal and humidity conditions that no condensation of water vapour occurs on the internal surfaces of building partitions. The phenomenon of moisture condensation on cold surfaces leads to windows fogging and, in the long term, to the weakening of building structural elements and the development of mould fungi.

Therefore, another purpose of thermal imaging research was to determine the risk of condensation of moisture on the internal surfaces of the windows, located in the south-western wall, as they were the coldest building elements. Under the prevailing conditions in the swimming pool: indoor air temperature t_i = 27.4°C, indoor air relative humidity ϕ_i = 56%, the corresponding dew point temperature was t_r = 17.9°C. This means that at a window temperature below 17.9°C, condensation of moisture contained in the air on its internal surface could occur.

The thermograms in Fig. 7 show temperature distribution on the internal surfaces of selected two windows O3 and O5 (Fig. 2). In order to detect areas at risk of moisture condensation, a dew point alarm was applied in FLIR Tools (right side of Fig. 7). This is the area marked green on the thermogram, whose temperature is lower than 17.9°C. On the thermograms made for all O1-O6 windows, measurement areas were introduced to determine the average temperature of the windows. Average temperature values ranged from 19.6°C to 25.3°C.

For most windows, the average temperature was similar, except for the O6 window, which had a temperature of 19.6°C. The reason for this was the turned-off radiator, located directly under the window, and the close vicinity of the second external wall. In case of all other windows, the radiators were on, which led to the increase of the windows temperature, as well as the external partition area. The average surface temperature values of the O1-O4 and O6 windows were higher than the dew point temperature, so there was no condensation at their entire surface. Only in case of the O5 window (Fig. 7b), there were areas where the temperature fell below the dew point and thus

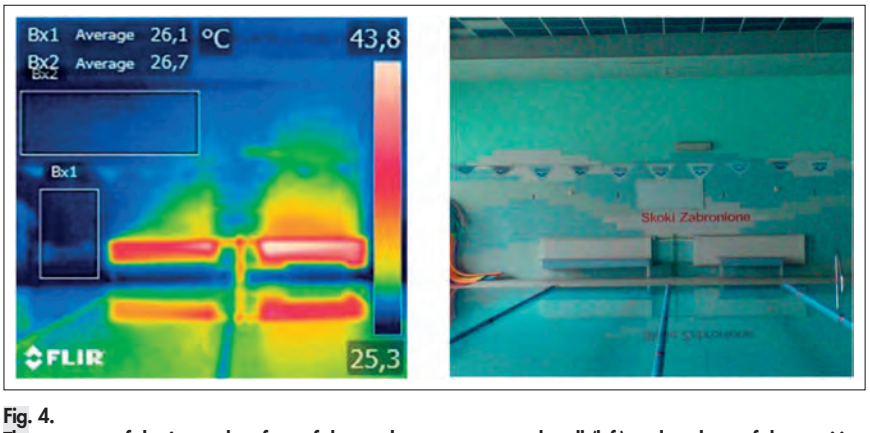

Fig. 4.
Thermogram of the internal surface of the north-western external wall (left) and a photo of the partition (right) [2]
Rys. 4. Termogram wewnętrznej powierzchni ściany zewnętrznej północno-zachodniej (po lewej) oraz zdjęcie przegrody (po prawej) [2]

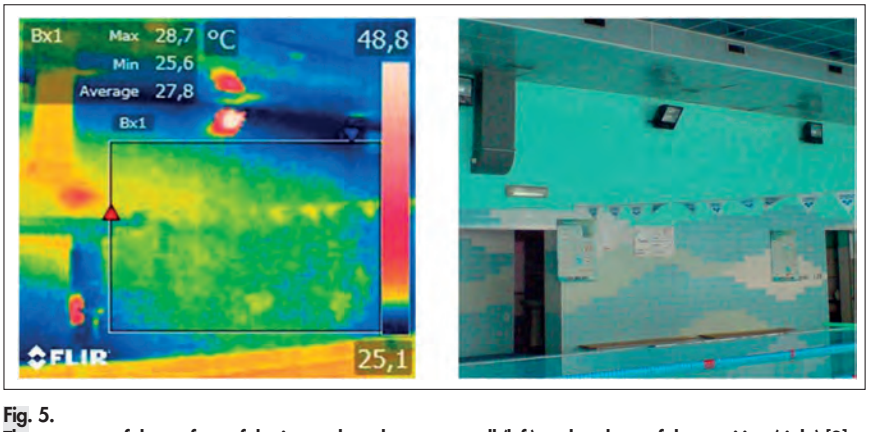

Fig. 5.
Thermogram of the surface of the internal north-eastern wall (left) and a photo of the partition (right) [2]
Rys. 5. Termogram powierzchni ściany wewnętrznej północno-wschodniej (po lewej) oraz zdjęcie przegrody (po prawej) [2]

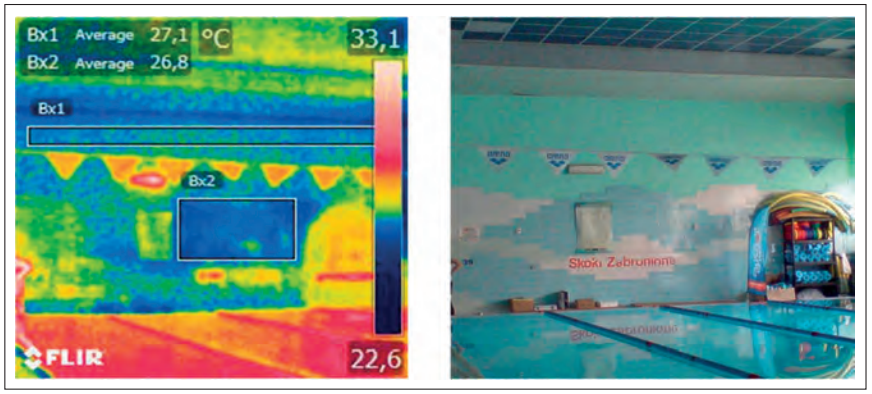

Fig. 6.
Thermogram of the surface of the internal south-eastern wall (left) and a photo of the partition (right) [2]
Rys. 6. Termogram powierzchni ściany wewnętrznej południowo-wschodniej (po lewej) oraz zdjęcie przegrody (po prawej) [2]

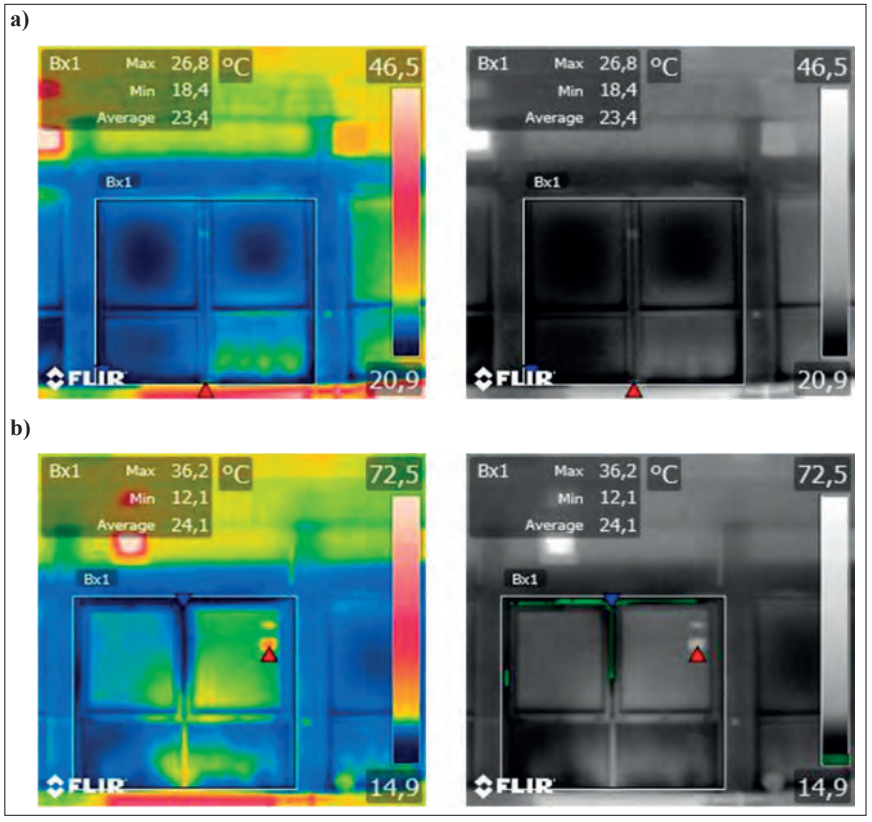

Fig. 7.
Thermograms of windows surfaces before applying the air dew point alarm (left) and after applying the air dew point alarm (right): a) window O3, where no moisture condensation occurred, b) window O5, where areas of moisture condensation occurred [2]
Rys. 7. Termogramy powierzchni okien przed wprowadzaniem alarmu punktu rosy (po lewej) i po wprowadzeniu alarmu punktu rosy (po prawej): a) okno O3, na którym nie wystąpiło wykroplenie wilgoci, b) okno O5, na którym wystąpiły obszary wykroplenia wilgoci [2]

the possibility of dampening the glass and the window frame appeared.

Based on thermographic images, it was found that the measured minimum surface temperature of five windows and other external building partitions was 18.4°C and was higher than the dew point temperature. This means that under measurement conditions there was no condensation on their surface.

Thermal imaging tests were carried out at outdoor air temperature t_e = 0.2°C, therefore the risk of moisture condensation on the surfaces of windows and building partitions was also assessed at outdoor air design temperature in climate zone III t_e = -20°C, according to the standard [16]. To convert the window surface temperature from the measurement values into values corresponding to the calculation conditions, the so-called law of temperature drop in the building envelope was used. It takes into account the proportional relationship between temperature drop and thermal resistance. At the same indoor air parameters, the minimum temperature of the indoor window surface would then be 11.5°C, so there would be a risk of moisture condensation on its surface. In case of other building partitions, there would be no condensation of moisture on their surfaces.

Calculation of thermal transmittance of external walls and windows in the swimming pool

Thermovision measurements of temperature distribution on internal and external surfaces of tested building partitions were also used to determine thermal transmittance of those partitions, the values of which were necessary to determine boundary conditions for numerical simulations. Calculation of thermal transmittance was carried out for two external walls: north-western and south-western, as well as for a window in the south-western wall. Thermograms of the external and internal surfaces of the examined partitions are shown in Fig. 8.

Fig. 8a shows thermograms of the external and internal surface of the north-western wall and in Fig. 8b thermograms of the external and internal surface of the south-western wall are shown. On the external surface of the south-western wall, the measuring area was applied below the window and on both sides of it. On the internal surface, the measuring area included the area on both sides of the window, as well as the area below the window, which was under the least influence of the radiator. Fig. 8c shows the thermogram of the window. The area in the lower part of the window covered with a matting film that could affect the results was omitted. In tab. 3 the average temperature values on both surfaces of the examined partitions were compared.

Tab. 3. Average temperature values on external and internal surfaces of the examined partitions [2]
Tab. 3. Średnie wartości temperatury na zewnętrznych i wewnętrznych powierzchniach badanych przegród [2]

Examined partition	The average temperature of the external surface of the partition, °C	The average temperature of the internal surface of the partition, °C
North-western external wall	0.3	26.4
South-western external wall	1.7	24.9
Window in the south-west wall	2.8	22.5

Based on the average values of temperature of external and internal surfaces of examined building partitions the thermal transmittance of these partitions was deter-

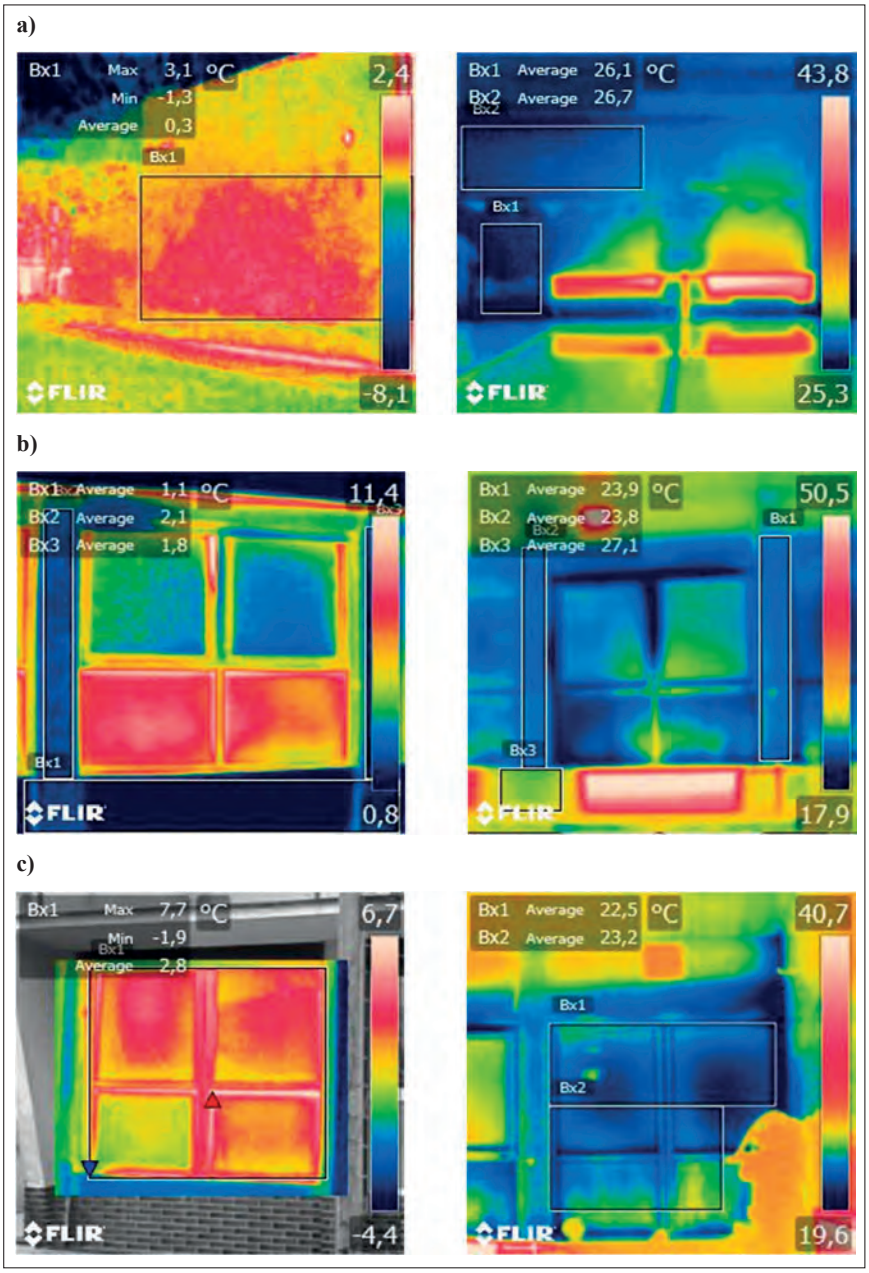

Fig. 8.
Thermograms of external surface (left) and internal surface (right): a) north-western external wall, b) south-western external wall, c) windows in south-western wall [2]
Rys. 8. Termogramy powierzchni zewnętrznej (po lewej) i powierzchni wewnętrznej (po prawej): a) ściany zewnętrznej północno-zachodniej, b) ściany zewnętrznej południowo-zachodniej, c) okna w ścianie południowo-zachodniej [2]

mined, which is given in Table 4. For this purpose, the methodology of calculation of thermal transmittance of building partitions described in Chapter 3.2 was applied.

Additionally, average values of thermal transmittance were compared with the results of calculations according to the standard [15], which were carried out on the basis of available data on the construction of building partitions obtained from partially outdated design documentation of the swimming pool, as well as from uncertain information obtained from technical services on the scope of thermal modernisation of the facility.

The results of these calculations are summarized in Table 5 and compared with the values calculated according to formulas (12) and (13) using thermographic measurements. The values of the thermal transmittance for both external walls are different because the north-western wall was insulated as part of the modernization of the swimming pool, while the construction of the south-westen wall was not changed since the construction of the swimming pool in the 1970s. The windows in the swimming pool were listed, but the value of their thermal transmittance was not known, so only the value obtained from thermovision measurements is given in Table 5. It can be seen that the results obtained from thermovision measurements were similar to those calculated on the basis of the construction design and information on the scope of thermomodernization of the facility. Both results, however, may be subject to errors. Therefore, for boundary conditions of numerical simulations [2, 4, 6] and energy analyses of ventilation processes in this building [5] average values of thermal transmittance of external walls determined by both methods were assumed. In the case of windows, the values calculated on the basis of thermovision measurements were assumed.

When comparing the values of the obtained thermal transmittance with those required from 1 January 2017, according to the Regulation [10], it can be seen that their values slightly exceed the values of U_{max} coefficients. For external walls at temperature $t_i \geq 16°C$ the maximum required value of thermal transmittance is currently $U_{max} = 0.22$ W/(m^2·K), which in the case of the north-western wall is almost fulfilled as $U_c = 0.223$ W/(m^2·K), whereas for south-western wall the permissible value was exceeded as $U_c = 0.340$ W/(m^2·K). The required thermal transmittance of the window should not currently exceed $U_{max} = 1.1$ W/(m^2·K), so the value obtained for the tested window $U_c = 1.522$ W/(m^2·K) exceeds the maximum value. Therefore, despite the replacement of windows during the modernisation of the building, the actual thermal transmittance does not meet the current requirements for U_{max} values.

Conclusions

1. The presented thermovision research was a part of wider experimental research on the parameters of air condition in the swimming pool, which was carried out using traditional measurement methods [3]. It turned out to be helpful in the assessment of thermal and humidity conditions occurring inside the examined facility and made it possible to determine the missing data concerning the values of thermal transmittance of building partitions.
2. The examination of the temperature distribution of the internal surface of the external partitions of the swimming pool using thermal imaging tests proved that their temperatures (26.4°C on the north-western wall and 24.9°C on the south-western wall) were significantly higher than the temperature of the dew point in the examined facility. Therefore, there

Tab. 4. Calculation results of external walls and windows thermal transmittance [2]
Tab. 4. Wyniki obliczeń współczynników przenikania ciepła ścian zewnętrznych i okien na podstawie pomiarów termowizyjnych [2]

Partition	Surface heat transfer coefficient, W/(m²·K)		Heat flux, W/m²	Thermal transmittance U, W/(m²·K)	Average thermal transmittance U_m, W/(m²·K)
	radiative	convective			
External wall, north-western					
– external surface	1.83	5.60	3.15	0.115	**0.200**
– internal surface	6.12	1.65	7.77	0.285	
External wall, south-western					
– external surface	1.34	5.60	8.81	0.330	**0.341**
– internal surface	6.09	1.75	9.41	0.352	
The windows in the south-western wall					
– external surface	1.91	5.60	39.21	1.469	**1.522**
– internal surface	5.98	2.78	42.05	1.575	

Tab. 5. Thermal transmittance of external walls and windows calculated by two methods [2]
Tab. 5. Współczynniki przenikania ciepła ścian zewnętrznych i okien obliczone dwiema metodami [2]

Calculation method	Calculated thermal transmittance *U*, W/(m²·K)		
	Wall NW	Wall SW	Window
Based on thermal imaging measurements	0.200	0.341	1.522
Based on the design project	0.245	0.398	-
Average value	0.223	0.340	1.522

was no risk of moisture condensation on their surfaces.

3. The examination of temperature distribution on the surfaces of six windows located in the south-western wall, using the dew point alarm, proved the presence of a small area with a minimum temperature of 12.1°C, lower than the dew point temperature, on one of the windows. This area was therefore exposed to condensation of moisture in the air. For the other five windows, a minimum temperature of 18.4°C was obtained, so there was no possibility of dampening the glazing and window frames.
4. The danger of condensation of moisture on the internal surfaces of all windows can occur at lower values of outdoor air temperature than those in which thermal imaging measurements were carried out (e.g. under calculation conditions). Eliminating this phenomenon is possible by increasing the volume flow of air supplied to the swimming pool through slot diffusers located under windows. Due to the induction of air from the interior of the swimming pool, the range of supply air jets can be improved, which will better protect the windows from condensation, as described in the paper [3].
5. Using thermal imaging tests and the calculation method described in Chapter 3.2 it is possible to determine thermal transmittance of building partitions, which is particularly useful in performing energy diagnostics of the building in case of lack or outdated building documentation.

REFERENCES

[1] Chludzińska, M. i Bogdan, A.(2010). Evaluation of the air flow from an individual ventilation diffuser using thermal imaging. Ciepłownictwo, Ogrzewnictwo, Wentylacja, 2, 31-34 (in Polish).
[2] Ciuman, P. (2017). Modeling the ventilation air distribution in the indoor swimming pool. Doctoral Dissertation, Gliwice: Silesian University of Technology (in Polish).
[3] Ciuman, P. (2020). Experimental assessment of thermal, humidity and flow conditions in the indoor swimming pool. Instal, 4, 32-38. DOI 10.36119/15.2020.4.6.
[4] Ciuman, P. and Lipska, B. (2018). Experimental validation of the numerical model of air, heat and moisture flow in an indoor swimming pool, Building and Environment, 145, 1-13.
[5] Ciuman, P., Lipska, B., Piękoś, K. and Trzeciakiewicz, Z. (2017). Impact of the supply air volume flow and heat recovery system on energy consumption in the ventilation process of the indoor swimming pool. Instal, 6, 39-45 (in Polish).
[6] Ciuman, P., Lipska, B., Trzeciakiewicz, Z. and Burda, G. (2015). Effect of the air volume flow on thermal comfort conditions in the school swimming pool. Instal, 11, 54-60 (in Polish).
[7] Górka, A. i Pawlak, F. (2015). Use of thermography to determine the range of the air jet. Rynek Instalacyjny, 5, 54-58 (in Polish).
[8] Kruczek, T. (2009). Determination of radiative ambient temperature during measurements in open air space. PAK vol. 55, 11, 882-885 (in Polish).
[9] Madura, H. i in. (2003). Thermal imaging measurements in practice. Warszawa: PAK (in Polish).
[10] Minister of Infrastructure RP. (2019). Regulation on the technical conditions to be met by buildings and their location (Journal of Laws pos. 1065) (in Polish).
[11] Neto, L.P.C. at all. (2006). On the use of infrared thermography in studies with air curtain devices. Energy and Buildings, 10, 1194-1199.
[12] Nowak, H. (2012). Application of thermal imaging tests in construction. Wrocław: Oficyna Wydawnicza Politechniki Wrocławskiej (in Polish).
[13] Palmowska, A. and Miczka, G. (2015). The usage of a thermal imaging camera to study the thermal and humidity conditions in indoor ice rink arena. Instal, 3, 44-49 (in Polish).
[14] Polish Standarization Committee [PKN] (2001). Thermal performance of buildings - Qualitative detection of thermal irregularities in building envelopes - Infrared method (Standard PN-EN 13187).
[15] Polish Standarization Committee [PKN] (2008). Building components and building elements - Thermal resistance and thermal transmittance - Calculation methods (Standard PN-EN ISO 6946).
[16] Polish Standarization Committee [PKN] (2006). Heating systems in buildings - Method for calculation of the design heat load (Standard PN-EN 12831).
[17] Collective work edited by Steidl, T. (2013). Guide to thermal diagnosis of buildings. Volume 1. In situ diagnostics of thermal insulation of buildings. NCBiR's strategic project "Integrated system to reduce the energy consumption of buildings in use". Gliwice: Silesian University of Technology (in Polish).
[18] Rymarczyk, Z. (2005). The use of thermography in energy audits of buildings. Conference materials from the 6th International Scientific and Technical Conference "Energy quality requirements for buildings by standardisation and development of energy carrier billing". Polańczyk (in Polish).
[19] Rymarczyk, Z. i Strzeszewski, M. (2004). Use of thermography to verify the numerical model of heat exchange in building partitions with central heating pipes. Conference materials from the 6th National Conference "Infrared Thermography and Thermometry". Ustroń-Jaszowiec,137-142 (in Polish).
[20] B. Więcek and G. De Mey (2011). Thermovision in infrared. Basics and applications. Warszawa: PAK (in Polish).
[21] http://tinyurl.com/pm5hyau
[22] www.flir.com

■